Design and fabrication of silica-based nanofiltration membranes for water desalination and detoxification

Design and fabrication of silica-based nanofiltration membranes for water desalination and detoxification

Ali Farsi[a], Camille Malvache[a], Onofrio De Bartolis[b], Giuliana Magnacca[b], Peter Kjær Kristensen[c], Morten Lykkegaard Christensen[a], Vittorio Boffa[a]

[a] Department of Chemistry and Bioscience, Aalborg University, Fredrik Bajers Vej 7H, DK-9220, Aalborg East, Denmark

[b] Università di Torino, Dipartimento di Chimica and NIS Centre, Via P.Giuria 7, 10125 Torino, Italy

[c] Department of Physics and Nanotechnology, Aalborg University, DK-9220, Aalborg, Denmark

ABSTRACT

Inorganic membranes typically have higher mechanical, thermal and chemical stability than their polymeric counterparts. Therefore, in this work a recent transport model was used to investigate the potential of porous inorganic membranes in water desalination. Salt rejection was predicted using the Donnan-steric pore model, in which the extended Nernst-Planck equation was applied to predict ion transport through the pores. The solvent flux was modeled using the Hagen-Poiseuille equation by considering the electroviscous effect. This model showed that inorganic NF membranes cannot achieve the selectivity of the traditional reverse osmosis (RO) membranes, and can only approach the perm-selectivity of the less robust but thinner and more flexible polymeric NF membranes. Nevertheless, inorganic NF membranes with pore size of about 1.5 nm and ζ-potential between 5 and 20 mV allow for a good compromise between water flux and salt rejection. Therefore, silica-based membranes with such properties were fabricated by sol-gel deposition. Since we have recently reported that the chemical and hydrothermal stability of unsupported microporous silica membranes can be highly enhanced by TiO2-doping, two sols were used for membrane deposition: a 5% TiO2-doped silica polymeric sol and a pure silica reference sol. The 5% TiO2-doped silica membrane showed water permeability (2.3 liters per square meter per hour per bar (LMH bar 1)) more than 30 times higher and higher salt selectivity than the pure silica membrane. As predicted by our model, at the 5% TiO2-doped silica membrane had approached without reaching salt rejection of commercial polymeric membranes with similar water flux, but it showed good performances when compared with the already reported inorganic NF membranes. Moreover, the new membrane presented nearly complete retention towards two model micropollutants, namely caffeine and ibuprofen. By investigating limits and potential of microporous inorganic mem-branes water desalination and detoxification, this work provides new knowledge for their rational design.

Keywords: Nanofiltration, Sol-gel, Desalination, Micropollutants, Silica

1. Introduction

As human population increases, water supplies become more limited and water scarcity is a serious global issue. In this context, there is a high demand for energy-efficient technologies for water softening, desalination, and detoxification. In particular, pressure-driven membrane processes provide relatively efficient and convenient means for achieving water purification [1,2]. Hydrated ions and organic micropollutants (e.g. pharmaceuticals, pesticides, hormones, etc.) have typically size smaller than 1 nm; therefore pressure-driven membrane technology for water desalination and detoxification is limited to reverse osmosis (RO) and nanofiltration (NF) membranes [3]. At the present RO by means of dense polymeric membranes is most common process for water desalination [1], since in principle it can remove all the dissolved ions from water. Solution-diffusion (SD) has emerged over the past decades as the most widely accepted transport mechanism in RO membranes [16]. On the contrary, NF membranes have typically pore size (pore diameter, dp) between 1 and 2 nm [17]. Rejection mechanisms are more complex [18]in NF membranes than in RO, because hydrated inorganic ions and most of the organic micropollutants are smaller than NF membrane pores. The selectivity of NF porous membrane depends on several factors like operation conditions (e.g. temperature, operating pressure), solution properties (e.g. concentration and type of ionic species), and membrane-solution interaction (e.g. membrane ζ-potential) [22-24]. NF membranes have lower ion rejection than RO membranes, but can offer several advantages such as low operating pressure and high permeability (L_p), resulting in relatively low investment, operation and maintenance costs [3]. NF membranes can reduce the concentration of monovalent ions (sodium, chloride, fluoride and nitrate), remove hardness, and remove small organics molecules from aqueous systems. Thus, NF membranes can be used as RO pre-treatment [19], for the direct production of drinking water from brackish water [20], and for the abatement of organic micropollutants in the water. At the present, RO and NF market is dominated by polymeric membranes. Table 1 reports desalination performances of some of these commercial membranes [4-15]. Polymeric membranes typically suffer from swelling, biofouling, scaling and poor thermal and chemical resistance [2,18,21], which limit their operation time and make difficult to clean them. In reason of that, inorganic NF membranes have been recently proposed as a possible alternative for water treatment [29-36]. Inorganic porous membranes have been widely utilized in practical areas including food processing, biotechnology, and petrochemical processing, because of advantages of process applicability such as thermal stability, resistance to solvents and chemicals, mechanical strength which enables inorganic membrane to work in harsh environments and under a wider pressure and pH ranges [25-28]. Full cleaning and regeneration is possible and hence longer membrane life time can be obtained [25,26]. However, inorganic membranes are expensive and will be commercially feasible in NF, only if they can reach perm-selectivity similar to their commercially polymeric counterparts. Table 2 reports literature results for inorganic NF and low-ultrafiltration (low UF) membranes in water desalination [29-36]. Among these membranes, MFI-type zeolite (silicalite) membranes showed good salt retention at low applied pressure (4-7 bar). However, they present also low

permeability (L_p < 0.1 LMH bar^{-1}) due to their small pore size and high membrane thickness (2-3 μm). Amorphous silica membrane structure has also been modified by inserting covalent organic bridges into the SiO_2 network. Pore size and thus perm-selectivity of these membranes can be tuned by adjusting the length of these organic bridges [37]. Xu et al. [31] have reported a L_p ~ 0.115 LMH bar^{-1} with R_{NaCl} > 89% for organosilica membrane (l ~ 0.2 μm) in ΔP = 7 bar. Organosilica membranes are typically thinner than zeolite membranes, but they are also denser and have a lower pore fraction, thus they also show low water permeability. Zirconia, titania, and alumina membranes have instead large pore size and thus show larger water permeability, but show NaCl rejection ≤ 52%. By comparing these results with those in Table 1, it is possible to see that inorganic porous membranes still present lower salt rejection than polymeric membranes with similar water permeability. Moreover, it should be stressed that the results in Table 2 were often obtained in strict laboratory condition for dilute NaCl solution (e.g. < 0.05 M) [29-36] and will probably show lower performances when used in real-scale filtration systems. This results can be explained by considering that the active layer of polymeric NF membranes consists of a 0.1-0.2 μm thick microporous polyamide, cellulose acetate or sulfonated polyethersulfone skin, and it is difficult to coat inorganic NF membrane layers with such thickness and with no defects. In this work, we use a recent-reported transport model [38] to investigate the potential of inorganic NF membrane in water desalination. The model was designed for inorganic membranes, which typically have a defined and rigid pore structure and high surface charge. In this work, new membranes were fabricated to validate the model and to assess their effective performances. Silica gel was selected as membrane materials since its surface charge at quasi-neutral pH matches the indications of our model and its pore size can be easily tailored by using surfactant micelles as sacrificial template. In a recent paper, we reported that pH-stability and hydrophilicity of unsupported silica membranes can be greatly enhanced by TiO_2 doping [39]. However, we also observed that the formation of a dense anatase phase appears to have a negative influence on the membrane pore volume and specific surface area, making the materials with a TiO_2 loading between 5% and 10% the most promising for membrane application. Following these findings, our recently reported synthetic path [39] was used to prepare a 5% TiO_2-doped silica sol and a reference silica sol. The two sols were coated over two commercial mesoporous γ-alumina/macroporous α-alumina tubes to from two NF membranes, which were tested for their water permeability and for their potential to remove NaCl, divalent ions, and model micropollutants from water.

2. Materials and methods

2.1. Transport modeling

Membrane permeability and salt rejection were studied ac-cording to our recently reported approach [38] based on optimized Donnan-steric pore model (DSPM). Salt rejection was predicted using the Donnan-steric pore model, in which the extended Nernst-Planck equation was applied to predict ion transport through the pores. The solvent flux was modeled using the Hagen-Poiseuille equation by introducing electro-viscosity instead of the bulk viscosity.

2.2. Sol-gel synthesis

The following reagents were used: tetraethyl-orthosilicate (TEOS, 99.0% Sigma Aldrich), titanium (IV) tetrabutoxide ($Ti(butO)_4$, 97%, Sigma Aldrich), ethanol (99.9% Kemityl), nitric acid (69% Sigma Aldrich), cetyltrimethyl ammonium (CTAB, Sigma Aldrich). Since $Ti(butO)_4$ is more sensitive to hydrolysis and condensation than TEOS, a two-step synthesis method was applied. In the first step, aqueous nitric acid was slowly dropped into a mixture of TEOS in ethanol under vigorous stirring to obtain the final molar ratio TEOS/ethanol/water/HNO_3 = 1/4/3/0.08. After stirring the mixture for 3 h at 60°C, the volume was adjusted with ethanol in a volumetric flask to obtain a final 1.5 M hydrolyzed-TEOS solution. A solution of $Ti(butO)_4$ in butanol (1 M) was prepared under inert atmosphere, and then added to the diluted hydrolyzed-TEOS under vigorous stirring at 5°C to obtain 5 mol% doping titania. The flask containing the mixture was heated at 60°C for 90 min under magnetic stirring. Then, 7.00 g of CTAB was added to mixture and the mixture was let to cool-down to room temperature (about 1 h) while stirring before membrane coating. A similar procedure was used to prepare a reference pure silica sol. In this case, an equivalent volume of pure butanol (with no $Ti(butO)_4$) was added to the pre-hydrolyzed TEOS mixture.

2.3. Membrane coating

The membranes were coated vertically on a lab-made machine at a dipping/withdrawing rate of 1.5 cm min^{-1}. An α-alumina supported g-alumina tubular membrane (250 x 10 x 7mm (L x OD x ID)) (Pervatech B.V., The Netherlands) was used as carrier. After coating, the membranes were dried at room temperature for 1 day and then calcined at 450°C for 3 h at a heating/cooling rate of 2°C min^{-1}.

2.4. Material characterization

Particle size measurements were performed on a Zetasiser NanoZS (Malvern). 20 mL aliquots of the two sols were dried in Petri-dishes in air and calcined at 450°C for 3 h at a heating/cooling rate of 2°C min^{-1}, that is, in the same conditions used for membrane fabrication. The presence of crystalline phases in these powders was investigated by XRD analysis using a PANalytical Empyrean diffractometer (PANalytical, Almelo, The Netherlands) with Cu Ka radiation. Pore size distribution, specific surface area, and pore fraction of the membrane material were determined by means of N_2 adsorption at liquid-nitrogen boiling point in a gas-volumetric apparatus ASAP2020 (Micromeritics, Norcross USA), after outgassing at 300°C in vacuum (residual pressure 10^{-2} mbar) for about four hours, that is, until no gaseous species arise from them. Porosity was obtained applying the Density Functional Theory (DFT) method on the adsorption branch of the isotherms [46]. High-resolution transmission electron microscopy (HRTEM)images were obtained on a JEOL 3010-UHR instrument (acceleration potential: 300 kV). Samples for TEM investigation were sup-ported onto holed carbon coated copper grid by dry deposition. The membrane composition and thickness of the TiO_2-doped silica active layer was determined by analyzing the cross-sectional view of the membrane a focused ion beam

scanning electron microscopes (FIB-SEM, Zeiss, EDX) at an accelerating voltage of 10 kV. The ζ-potential of TiO_2-doped silica particles was measured as a function of pH using a Zetasizer (Nano NS, Malvern, UK). The solution pH was increased by adding KOH (Sigma Aldrich) steadily by an auto-titrator (Malvern MPT-2). The suspensions contained 20 mL of 10 mM NaCl in deionized water (Milli-Q produced by Nanopure Dimond, 18.2 MΩ cm) in which 20 mg TiO_2-doped silica particles was dispersed by ultrasonic treatment and remained 24 h at room temperature.

2.5. Filtration experiments

Deionized water (Milli-Q produced by Nanopure Dimond,18 MΩ cm) was used in all the filtration experiments. Inorganic and organic solutes were purchased by Sigma-Aldrich: NaCl (purity > 99.5%), Na_2SO_4 (> 99.5%), $MgCl_2.6H_2O$ (> 99.0%), $MgSO_4.7H_2O$ (> 99.0%), $CaCl_2.2H_2O$ (> 99.0%), and $CaSO_4\$2H_2O$ (> 99.0%), $CuCl_2.2H_2O$ (> 99.0%), ibuprofen (≥ 98%), and caffeine (> 99.0%). A previously reported cross-flow filtration set-up [24] was used for this study. Inorganic salt solutions were prepared all with an ionic strength of 0.01 M. The system was operated for 2 h to ensure that the membrane surface was in equilibrium with solution and the system was at the steady state condition. The applied pressure (ΔP) was set to 6 bar for all experiments. The cross-flow rate was maintained at 0.75 L min^{-1} to provide a cross-flow velocity of approximately 20 m/s. Such velocity is far from real life situations (cross-flow velocity typically smaller than 2 m/s), but was used to reduce concentration polarization phenomena [24,40], which were not considered by our model. The salt rejection $R = 1 - (c_{permeate}/c_{feed})$ was determined by measuring conductivity of feed and permeate using a conductivity meter (SevenMulti™ S70-K bench-top, Switzerland with ± 0.5% accuracy). The ionic strength was 0.01 M for the feed solutions and < 0.01 M for all the permeates; thus, concentration was considered as a linear function of conductivity [24,33]. A feed solution with caffeine (1 ppm) and ibuprofen (1 ppm) was prepared and used for membrane retention tests. Caffeine and ibuprofen concentration in the retentate and in permeate was determined by HPLC over a Dionex ASI-100 chromatograph with a UV detector (A Phenomenex Luna C18 column; with diameter, length, and pore size of 4.60 mm, 250 mm, and 5mm, respectively). The mobile phase was deionized water (buffered with 0.025 M KH_2PO_4) and acetonitrile (ACN), with a proportion ACN/buffer of 60/40 for ibuprofen and 20/80 for caffeine, delivered at a flow rate of 1 mL min^{-1}. Membrane support was also tested in the same conditions for comparison and to determine the active layer permeability by using the resistance-in-series theory [40].

3. Results and discussion

3.1. Potential of inorganic NF membranes in water desalination. The first objective of this paper is to investigate the potential of inorganic NF membranes in water desalination, also in comparison with commercial polymeric RO or NF membranes. To achieve this goal we used the recent reported optimized Donnan-steric pore model (DSPM) for NF and UF membranes [24]. In this model, the modified Hagen-Poiseuille equation predicts solvent flux

$J_p = (d_p^2\varepsilon)/(32\ \eta_{app}\tau l)\ (\Delta P-\Delta\pi)$, where d_p is membrane pore size, η_{app} is solvent viscosity in the membrane pore, ε is membrane porosity and τ is membrane tortuosity [24,40]. The ion separation is described by a coupling between the hindered transport inside the pore governed by a combination of convection, diffusion and electromigration terms (electrical potential gradient) and the equilibrium partitioning at the membrane/solution interfaces governed by Donnan, steric, dielectric interfacial exclusion mechanisms [22,24]. In the DSPM model, the pressure difference produces a smooth gradient in pressure through the membrane [24,38,41]. The assumptions of DSPM model are acceptable for the membranes with pore size larger than ions (d_p > 0.5 nm)[41]. The model is designed for oxide (silica and ceramic) membranes, which compared to polymeric membranes have high surface charge and a defined and rigid pore structure. Fig. 1a shows the simulation of NaCl rejection (R_{NaCl}) by microporous and mesoporous membranes with 0.5 nm < d_p < 8 nm and 0 < $|\zeta|$ < 50 mV. The bulk feed concentration and applied pressure were considered to be 10 mM (NaCl ~ 0.6% wt) and 6 bar, respectively. In this concentration, the osmotic pressure differences (Δp) is less than 0.3 bar [24,40]. The hydration diameters (d_s) of Na^+ and Cl^- were considered 0.37 and 0.24 nm, respectively [24,41,42]. As obvious, ion rejection increases by decreasing the pore size, due to steric exclusion at the membrane/solution interfaces. This effect is more evident for no charged membranes (z¼0). The ζ-potential increases the volume charge density and electroviscous effect in the pore, simultaneously. Ions moving along the electric field generated by the streaming potential will drag solvent molecules within membrane pores, thus increasing the apparent viscosity of the liquid. This phenomenon is commonly named electroviscous effect[24]. The volume charge density increases the ion rejection because of both interfacial exclusion and electromigration (caused by electrical potential gradient); while the electroviscous effect decreases the ion rejection in result of flux decline. These opposite effects, namely ζ-potential increasing the electromigration term and decreasing the convection term, cause an optimum ζ-potential for salt rejection, which is indicated by R_{max} in Fig. 1a. This maximum is evident for nanoporous membranes with d_p <6 nm. The ζ-potential of optimum rejection decreases with increasing d_p and also depends on the nature of the ions [38]. According to Fig.1a, R_{NaCl} > 85% can be obtained solely by nanoporous membranes with d_p of 0.5 nm or smaller and $|\zeta|$ > 10 mV. For practical applications, a membrane should combine high selectivity and high permeability. For this reason, the simulation of NaCl rejection and membrane permeability of membranes with 0.5 nm < d_p < 10 nm and 0 < $|\zeta|$ < 60 mV is depicted Fig. 1b. The membrane thickness (l) was considered to be 1 μm. Effect of membrane thickness on membrane permeability is indicated by the horizontal black lines for 0.2 μm < l < 2 μm. It is worth to mention that depositing and calcining defect-free ceramic or silica layers with l < 0.2 μm on large-area porous carriers is technically challenging with the commonly used methods in membrane preparation, like slip casting, tape casting, and dip coating [43]. In this simulation, membrane porosity (ε) was considered to be 0.5 and it was assumed that the membrane tortuosity (τ) was equal to 3 for all active layers, similar to values reported in the literature. [44e46].Fig. 1b indicates that membrane permeability increases with pore size and decreases with the ζ-potential. This is

consistent with literature data reported in Table 2. For instance, silicalite membranes showed NaCl rejection of 47-72% mainly because of low ζ-potential (~ 5 mV at pH = 6-7), but Li et al.[25]has increased the ζ-potential of MFI-type zeolite membrane by increasing theratio of Si/Al (|ζ| > 50 mV) achieving approximately 90% of NaCl rejection for a membrane with L_p of 0.005 LMH bar^{-1}. In general, the values reported in Fig. 1b have a good correspondence with the data in Table 2, despite the difference in membrane composition and test conditions. Fig. 1b indicates that porous membranes with d > 2 nm are not capable to remove more than 45% of NaCl. Indeed, excluding a few papers [47,48], which report filtration experiments conducted on unconventional conditions, mesoporous oxide membranes, such as γ-alumina, titania and zirconia with d_p > 2 nm, are not able to remove more than 40% NaCl. Our model also shows that theoretically inorganic porous membranes with pore size of 0.5 nm (e.g. zeolite and organosilica) can achieve the same perm-selectivity of dense polymeric RO membrane for water desalination unless membrane thickness would be technically reduced to be less than 50 nm which is hard to obtain with the current coating technologies[31,43]. On the other hand, Fig. 1b suggests that membranes should have a pore size in the 1-2 nm range and |ζ| between 5 and 20 mV to achieve NaCl rejection > 50%. Under this conditions, L_p > 1 LMH bar^{-1} can be obtained with a layer with thickness of 2 μm while deposition of a thin layer (e.g. 200 nm) can provide L_p > 10 LMH bar^{-1}.

3.2. Membrane materials: morphology and surface charge

Herein, we report two new inorganic NF membranes within the mentioned pore size and optimum ζ-potential over a broad pH interval. Silica is an ideal material for the fabrication of such membranes, since silica surface is known to be negatively charged at pH above 2-2.5 [49], and high pore volume and pores size in 1-2 nm range can be attained by means of cetyl-trimethylammonium bromide (CTAB) micelles as sacrificial template[50e53]. As mentioned in the Introduction paragraph, the membranes were prepared by sol-gel deposition over commercial supports. Two sols were used for membrane coating: a pure silica sols and a 5% TiO_2-doped silica sols, since we have recently showed that TiO_2-doping can increase pH-stability and hydrophilicity of unsupported silica membranes [39]. Particle size distributions of the sols were measured before CTAB addition, in order to check if the colloids have size adequate to coat a thin microporous membrane over a mesoporous support, as required for the target NF membrane. Fig. 2 shows that solvated particles of the undoped and TiO_2-doped silica sols have size distributions with a maximum at about 2 and 5 nm, respectively. The fact that the TiO_2-doped sol has larger particle size compared to the pure silica one, is common for transition metal doped silica sol [54-56] and is consistent with the high reactivity of the transitionmetal alkoxide used as precursor. The particle size of both sol is suitable for the surfactant-templated method[58]. However, the particles of the pure silica sol are rather small and they may penetrate in the pores of the mesoporous carrier used as membrane support. Fig. 3a and 3c show the TEM images of the heat-treated un-supported pure silica and 5% TiO_2-doped silica membranes. The membrane materials appear to be fully amorphous and homogeneous with

disordered pore structure. The absence of long-range order in both samples was confirmed by the absence of peaks in the X-ray diffractograms (both at $2\theta > 5°$ and at $2\theta < 5°$), which are not reported here for the sake of briefness. This result indicates that the procedure used in this study allowed for a good dispersion of the Ti^{4+} ions in the amorphous silica matrix and lead to the formation of a disorder porous structure. This observation might be explained by considering that the use of a mixture of butanol and ethanol as solvent has probably hindered the formation of an ordered micelle structure during the consolidation of the material before calcination. The pore size distribution of the two materials was measured by low temperature nitrogen adsorption. As shown in Fig. 3b and 3d,most of the nitrogen is adsorbed at a relative pressure < 0.2 and the sorption curve has a plateau for higher relative pressure. This sorption isotherm corresponds to the Type I of IUPAC classification[59], which is typical of systems with micropores and/or small mesopores. The pore size distributions show indeed that both membranes have pores with size smaller than 2.5 nm with an average size between 1 and 2 nm. Moreover, both materials show high specific surface area (981 and 863 m^2g^{-1}, respectively) and high pore fraction ($\varepsilon = 0.73$ and $\varepsilon = 0.71$, respectively), as typical for surfactant template silica structures which is consistent with the use of CTAB micelles as structure directing agents[49,50]. The ζ-potential of the pure silica and of the 5% TiO_2-doped silica layer was measured on unsupported membrane particles dispersed in an aqueous solution of different inorganic salts (ionic strength0.01 M) over a pH range between 1.7 and 6, as shown in Fig. 4.Dissolved salts have little effect on the surface charge of both materials, whose isoelectric point lays in between pH 2 and 3, as typical for silica powders. The change of dissolved salts produce only a little shift in the isoelectric point from pH ~ 2 to higher pH, according to the order: $CaSO_4 < Na_2SO_4 < NaCl < MgCl_2 < CaCl_2$, indicating that sulphate ions and divalent cations have only weak or extremely weak interactions with the material surface. This trend is more pronounced for the TiO_2-doped silica sample. However, the influence of dissolved salts on ζ is far what has been observed for γ-alumina support material[24,38]. In our case, both membrane materials are negatively charged when exposed at a solution with pH above 3 and the condition $5 < |\zeta| < 20$ mV, i.e. ζ-potential favorable for ion rejection, is verified for many water systems.

3.3. Membrane structure and water permeability

Two NF membranes were fabricated by coating the pure silica and the 5% TiO_2-doped silica colloids on two commercial γ-alumina/α-alumina tubular carriers. The SEM cross-section images of the two supported membranes are depicted in Fig. 5. This picture shows the defect-free TiO_2-doped silica layer deposited on the mesoporous (pore diameter ~ 5.5 nm) γ-alumina interlayer. A thickness (l) of 1.2 μm was measured for both the membrane top-layers. The composition of the TiO_2-doped silica layer was analyzed by EDX showing a Ti/(Ti + Si) molar ration of 5 ± 2%, which is consistent with the composition of the sol used for membrane coating. Water permeability of the two membranes was tested with deionized water (18 MΩ cm) at ΔP of 6 bar. The 5% TiO_2-doped silica membrane showed a water permeability of $L_p = 2.3$ LMH bar^{-1}, i.e. more than one order of magnitude higher than the pure silica membrane, which

has $L_p = 6.3 \cdot 10^{-2}$ LMH bar^{-1}. Fig. 6 shows the resistances of membrane top-layers and support against water flux. The resistance of the TiO_2-doped silica layer is comparable with that of the support, thus making this membrane interesting for practical applications if achieving higher selectivity than the support γ-alumina/α-alumina tube. By subtracting the support and interlayer effects on the permeability using the resistance-in-series theory [38], the active layer permeability (TiO_2-doped silica) was determined to be approximately 3.1 LMH bar^{-1} which can be expected from a layer with d_p = 1.44 nm, l > 1.87 μm, ε = 0.71 and tortuosity (τ) correspondent to 2.1. Such tortuosity is consistent with the disordered arrays of micropores in the membrane layer. On the contrary, the resistance against water flux of the pure silica membrane is two orders of magnitude higher than that of its support, thus this membrane appears not be suitable for real filtration systems. This result is surprising, since the two membrane materials have similar pore structure and surface charge. TiO_2-doped silica membranes have been reported to be more hydrophilic than pure silica [39], but this feature cannot justify such a difference in water permeability. On the other hand, the particle size of the sol used for the coating of the pure silica membrane is markedly smaller than the size of the 5% TiO_2-doped silica sol particles. Therefore, the scarce water permeability of the pure silica mem-brane can probably be ascribed to the penetration and partial occlusion of the γ-alumina support mesopores by the unreacted TEOS and the silica clusters, as already observed for other membranes [56,57].

3.4. Desalination

The transport model [38] was verified by filtering NaCl solutions(ionic strength 0.01 M) in the pH range 2.0-7.8 over the 5% TiO_2-doped silica membrane. Water permeability data are depicted as a function of ζ in Fig. 7a, together with the trend predicted by our transport model. In general, the experimental values are close to our simulation and the general trend of a slight reduction of the membrane permeability at high $|\zeta|$ due to the electroviscous effect is verified. Fig. 7b reports NaCl rejection as a function of $|\zeta|$. As predicted by our model, the lowest rejection was observed at low pH where $|\zeta|$ < 10 mV, in accordance with a rejection mechanism dominated by Donnan exclusion: the Derby length (double layer thickness) is 3 nm for 0.01 M NaCl, and thereby fill out the mem-brane pores. Thus, negatively charged ions are excluded from the pores. The ion exclusion is more pronounced for highly charged pores (high $|\zeta|$).Filtration tests over the pure silica membrane were made difficult by its low water permeability. Indeed, several hours were necessary to be able to collect the minimum volume of permeate(10 mL) that is required for the conductivity analysis. Despite that, the ability of the pure silica membrane to reject salts of mono-valent and divalent ion was investigated, in order to appreciate the selectivity of the TiO_2-doped silica membrane. Thus, salt rejection of the two new NF membranes was measured for NaCl Na_2SO_4,$MgCl_2$, $MgSO_4$, $CaCl_2$, and $CaSO_4$ solutions (ionic strength 0.01 M in deionized water with no pH correction,DP¼6 bar), and compared to that of the γ-alumina support in Fig. 8. The γ-alumina support (d_p = 5.5 nm) showed rejection values of 23% for NaCl, 32% for Na_2SO_4, about 40% for $MgCl_2$ and $CaCl_2$, and about 50% for

$MgSO_4$ and $CaSO_4$. The high rejection of sulphate salts by γ-alumina membrane has been suggested to be caused by the adsorption of divalent ions on the membrane pore wall, which might facilitate steric exclusion[38]. The TiO_2-doped silica membrane had always higher salt rejection than the γ-alumina support, indicating that no significant defects were present in the new NF layer. A rejection of 58% was measured for NaCl, and rejection values between 60% and 70% was measured for the other salts. Ion rejection is expected to be higher for the microporous silica-based membrane than for the mesoporous γ-alumina, because of the smaller pore size. Moreover, the difference of rejection for the different salts is smaller for the TiO_2-doped silica membrane than in the γ-alumina support, for which $MgSO_4$ and $CaSO_4$ rejections were more than two fold higher than NaCl rejection). This is consistent with the weak interaction of the silica membrane with the dissolved ions(Fig. 4). The pure silica NF membrane had a rejection of 34% and44% for NaCl and Na_2SO_4, respectively. The rejection of these two salts was higher than that of the bare support, indicating that a continuous silica layer was formed, but the rejection ability of this layer was lower than the one of the TiO_2-doped silica membrane. Moreover, the rejection of pure silica membranes for the other four salts was not significantly different from that of the γ-alumina support. Since the TiO_2-doping appeared to have no significant impact on the pore size (Fig. 3) and on the ζ-potential (Fig. 4) of the membrane material, the difference in performances between the two membranes should be related to the quality of the pure silica membrane layer and to its scarce permeability:

3.5. Pollutant removal

The two new NF membranes were tested also for their ability to remove a potentially toxic inorganic pollutant, copper (Cu^{2+}) [61], and two model organic pollutants, namely caffeine ($C_8H_{10}N_4O_2$, Mw = 194.19 g/mol) [62] and ibuprofen ($C_{13}H_{18}O_2$, Mw = 206.29 g/mol) [63], and compared to the bare support. Retention values are reported in Fig. 9. The bare γ-alumina support and the two membranes showed a $CuCl_2$ rejection similar to that observed for $MgCl_2$ and $CaCl_2$. This can be explained by considering that Cu^{2+} has the same net charge and similar size of the Mg^{2-} and the Ca^{2+} ions. On the contrary, the three membranes had a highly different rejection of the organic micropollutants. The bare support, the pure silica membrane and the TiO_2-doped silica membrane respectively showed a rejection of 5%, 77%, and 91% for ibuprofen, and of 3%, 85%, and 90% for caffeine. This observation can be explained considering that the steric exclusion is the main rejection mechanism for these neutral organic molecules, resulting in much higher rejection for the new NF silica membrane (pore size ~ 1.4 nm) than for the γ-alumina support (pore size ~ 5.5 nm). These data confirm that the pure silica membrane consisted of a continuous selective layer. Moreover, they show that the TiO_2-doped silica membrane can combine water permeability and selectivity values for ibuprofen and caffeine comparable to those reported for commercial polymeric NF membranes [64-66].

4. Conclusions

This study had the following objectives: (i) to model the potential of inorganic NF membranes in water desalination, (ii) to design and fabricate new inorganic membranes on the basis of the simulation results, (iii) to test the new membranes, in order to validate the model and to assess their potential in desalination and detoxification of water systems. Our model showed that a combination of water permeability and NaCl rejection close to that of commercial dense polymeric RO membranes can be potentially achieved by solely membranes with pore size (d_p) < 0.5 nm and thickness (l) < 50 nm (pore fraction ε = 0.5). However, the coating of such thin membranes is hard to achieve without defect over large filtering areas. On the contrary, the model suggested that membranes with a mean pore size be-tween 1 and 2 nm and $5 < |\zeta| < 20$ can potentially approach the perm-selectivity of commercial polymeric NF membranes. There-fore, we fabricated a pure silica membrane and a TiO_2-doped silica membrane with the above mentioned properties. Despite the two materials were synthetized in similar conditions, the higher reactivity of $Ti(Obut)_4$ cause the TiO_2-doped silica sol to have larger particle size than the pure silica sol. Nevertheless, after drying and calcination the two materials showed similar pore structure and surface properties, as revealed respectively by nitrogen adsorption analysis and ζ-potential measurements. Thus, the two membrane materials were coated over γ-alumina/α-alumina tubes and tested in a cross-flow filtration apparatus at an applied pressure of 6 bar. The water permeability of the pure silica membrane was lower than $7 \cdot 10^{-2}$ LMH bar^{-1}, i.e. far below the permeability of commercial membranes, while the 5% TiO_2-doped silica membrane showed a water permeability of 2.3 LMH bar^{-1}, which is interesting for practical application. Hence, the size of the coating sol is confirmed to play a key role in the membrane resistance, e.g. by preventing penetration in the support mesopores. In good agreement with our model, desalination tests showed that the 5% TiO_2-doped silica membrane removed approximately 59% of NaCl at pH ~ 6; while at pH ≤ 4, NaCl rejection decreased, because of the low $|\zeta|$. Higher rejection values (between 60% and 70%) were observed for salts of divalent cations and/or anions at quasi-neutral pH. The selectivity of the new 5% TiO_2-doped silica membrane is higher than that of the bare support and it is also less affected by the feed composition (a feature desirable for practical water filtrations, which can imply fluctuations in the feed solution).As predicted by our model, in terms of NaCl rejection and water permeability, the 5% TiO_2-doped silica membrane can only approach the thinner polymeric NF membranes (Table 1,200 < MWCO < 400 Da, in operation condition of ΔP = 4-10, T = 20-30°C and pH = 5-7). However, most of the reported alumina, titania and zirconia membranes have a salt rejection lower than the 5% TiO_2-doped silica membrane presented this work. Higher salt rejection can be achieved by other silica-based mem-brane such as silicates and hybrid organo-silica membranes, which however have water permeability more than 20 times lower than our membrane. Moreover, the new TiO_2-doped silica membrane showed nearly complete retention towards caffeine and ibuprofen, i.e. much larger than the mesoporous support. Hence, our simulations and experimental results call in to question the possibility of inorganic NF membrane to reach the desalination performances of the commercial polymeric RO and NF membranes. Nevertheless, our results confirm their ability to retain > 50% NaCl and other salts, and their high potential in

micro-pollutants removal. These features, together with their good chemical and hydrothermal stability, make these membranes interesting for various applications as RO pre-treatment units and for those NF applications requiring frequent cleaning or sterilization cycles. By investigating limits and potential of inorganic NF membranes in water desalination and detoxification, this work provides new knowledge for their rational design.

Acknowledgements

This research was supported by grants from the Danish National Advanced Technology Foundation (project 0-59-11-1) and by the European Union's Horizon 2020 research and innovation pro-gramme (Marie Skłodowska-Curie grant agreement n. 645551).

References

[1]A. Shrivastava, S. Rosenberg, M. Peery, Energy efficiency breakdown of reverse osmosis and its implications on future innovation roadmap for desalination, Desalination 368 (2015) 181-192.

[2]M.A. Shannon, P.W. Bohn, M. Elimelech, J.G. Georgiadis, B.J. Marinas, A.M. Mayes, Science and technology for water purification in the coming decades, Nature 452 (2008) 301-310.

[3]C.K. Diawara, Nanofiltration process efficiency in water desalination, Sep.Purif. Rev. 37 (2008) 302e324.

[4] FILMTEC™XLE-2521 Membranes, Form No. 609-00349-0706.www.lenntech.com/Data-sheets/Dow-Filmtec-XLE-2521.pdf.

[5] FLUID SYSTEMS®TFC®-ULP®4”ELEMENT, KOCH membrane system,www.lenntech.com/Data-sheets/Koch-Fluid-Systems-TFC-4040-ULP-L.pdf

6] Toray Membrane Product,www.toraywater.com/products/ro/pdf/TMG.pdf.

[7] Hydranautics Corporatehttp://www.membranes.com/docs/4inch/ESPA4-4040.pdf.

[8] AK Series Low Energy Brackish Water RO Elements, GE water&processtechnology,http://www.lenntech.com/Data-sheets/GE-Osmonics-AK-series-Low-Energy-Brackish-Water.pdf.

[9] FILMTEC™Membranes, FILMTEC NF270 Nanofiltration Elements for Com-mercial Systems, Form No. 609-00519-1206,http://www.lenntech.com/Data-sheets/Dow-Filmtec-NF270-2540.pdf.

[10] FILMTEC Membranes, Nanofiltration Produces Sparkling Clean Water forSwedish Resort Community, Form No. 609-00379-0503, http://msdssearch.dow.com/PublishedLiteratureDOWCOM/dh_0047/0901b803800478f5.pdf?filepath=liquidseps/pdfs/noreg/609-00379.pdf&fromPage=GetDoc.

[11] FILMTEC™Membranes, FILMTEC NF90e400 Nanofiltration Element, Nano-filtration Elements for Commercial Systems, Form No. 609-00345-0406,http://www.lenntech.com/Data-sheets/Dow-Filmtec-NF90-400.pdf.

[12] CK Series, Water Softening NF Elements (Cellulose Acetate), GE water&process technology,https://www.gewater.com/kcpguest/salesedge/documents/Fact%20Sheets_Cust/Americas/English/FS1268EN.pdf.

[13] Hydranautics Corporatehttp://www.membranes.com/docs/8inch/ESNA1-LF-LD.pdf.

[14] TS80 Nanofiltration Element Series, TriSep Corporation,http://membranes.trisep.com/Asset/8040-TS80-TSA-spec-sheet.pdf.

[15] Product Guide for Spiral-Wound RO&NF Elements, CSM,http://www.csmfilter.com/csm/upload/RO_Catalogue/CSM%20RO%20Catalog_Eng_Final_DavidK_11.7.12.pdf.

[16]J.G. Wijmans, R.W. Baker, The solution-diffusion model: a review, J. Membr.Sci. 107 (1995) 1-21.

[17]B. Van der Bruggen, M. Manttari, M. Nystrom, Drawbacks of applying nano-filtration and how to avoid them: a review, Sep. Pur. Technol. 63 (2008) 251-353.

[18]B. van der Bruggen, J. Geens, in: N.N. Li, A.G. Fane, W.S. Winston Ho,T. Matsuura (Eds.), Nanofiltration, Advanced Membrane Technology and Applications, John Wiley&Sons, 2008, pp. 271-295.

[19]L. Malaeb, G.M. Ayoub, Reverse osmosis technology for water treatment: state of the art review, Desalination 267 (2011) 1-8.

[20]A. Lhassani, M. Rumeau, D. Benjelloun, M. Pontie, Selective demineralization of water by nanofiltration application to the defluorination of brackish water, Water Res. 35 (2001) 3260-3264.

[21]S. Duscher, Ceramic membranes for thefiltration of liquids: an actual over-view, Filtr. Sep. Intern. 14 (2014) 13-21.

[22]S. Deon, P. Dutournie, P. Bourseau, Transfer of monovalent salts through nanofiltration membranes: a model combining transport through pores and the polarization layer, Ind. Eng. Chem. Res. 46 (2007) 6752-6761.

[23]J. Benavente, V. Silva, P. Pradanos, L. Palacio, A. Hernandez, G. Jonson, Com-parison of the volume charge density of nanofiltration membranes obtained from retention and conductivity experiments, Langmuir 35 (2010) 11841-11849.

[24]A. Farsi, V. Boffa, H.F. Qureshi, A. Nijmeijer, L. Winnubst, M.L. Christensen,Modeling waterflux and salt rejection of mesoporous γ-alumina and micro-porous organosilica membranes, J. Membr. Sci. 470 (2014) 307-315.

[25]T. Tsuru, Inorganic porous membranes for liquid phase separation, Sep.Purific. Method 30 (2001) 191-220.

[26]Y.S. Lin, Microporous and dense inorganic membranes: current status and prospective, Sep. Pur. Technol. 25 (2001) 39-55.

[27]K. K€onig, V. Boffa, B. Buchbjerg, A. Farsi, M.L. Christensen, G. Magnacca, Y. Yue, One-step deposition of ultrafiltration SiC membranes on macroporous SiC supports, J. Membr. Sci. 472 (2014) 232-240.

[28]M. Facciotti, V. Boffa, G. Magnacca, L.B. Jørgensen, P.K. Kristensen, A. Farsi, K. Konig, M.L. Christensen, Y. Yue, Deposition of thin ultrafiltration mem-branes on commercial SiC microfiltration tubes, Ceram. Int. 40 (2014) 3277-3285.

[29]L. Li, N. Liu, B. McPherson, R. Lee, Enhanced water permeation of reverseosmosis through MFI-type zeolite membranes with high aluminum contents, Ind. Eng. Chem. Res. 46 (2007) 1584-1589.

[30]B. Zhu, D.T. Myat, J.W. Shin, Y.H. Na, I.S. Moon, G. Connor, S. Maeda, G. Morris,S. Gray, M. Duke, Application of robust MFI-type zeolite membrane for desalination of saline wastewater, J. Membr. Sci. 475 (2015) 167-174.

[31]R. Xu, J. Wang, M. Kanezashi, T. Yoshioka, T. Tsuru, Reverse osmosis performance of organosilica membranes and comparison with the pervaporation and gas permeation properties, AICHE 59 (2013) 1298-1307

[32]T. Van Gestel, C. Vandecasteele, A. Buekenhoudt, C. Dotremont, J. Luyten,R. Leysen, B. Van der Bruggen, G. Maes, Salt retention in nanofiltration withmultilayer ceramic TiO_2 membranes, J. Membr. Sci. 209 (2002) 379-389.

[33]P. Puhlfürß, A. Voigt, R. Weber, M. Morbe, Microporous TiO_2 membranes with a cut off<500 da, J. Membr. Sci. 174 (2000) 123-133.

[34]Y. Cai, Y. Wang, X. Chen, M. Qiu, Y. Fan, Modified colloidal sol-gel process for fabrication of titania nanofiltration membranes with organic additives, J. Membr. Sci. 476 (2015) 432-441.

[35]H. Qi, G. Zhu, L. Li, N. Xu, Fabrication of a sol-gel derived microporous zirconiamembrane for nanofiltration, J. Sol-Gel Sci. Technol. 62 (2012) 208-216.

[36]J. Schaep, C. Vandecasteele, B. Peeters, J. Luyten, C. Dotremont, D. Roels, Characteristics and retention properties of a mesoporousg-Al2O3membranefor nanofiltration, J. Membr. Sci. 163 (1999) 229-237.

[37]R. Xu, J. Wang, M. Kanezashi, T. Yoshioka, T. Tsuru, Development of robust organosilica membranes for reverse osmosis, Langmuir 27 (2011) 13996-13999.

[38]A. Farsi, V. Boffa, M.L. Christensen, Modelling water permeability and salt rejection of mesoporous γ-alumina nanofiltration membrane in a broad pH range, ChemPhysChem 16 (2015) 3397-3407.

[39]V. Boffa, L. Parmeggiani, G. Magnacca, Hydrophilicity and surface heterogeneities of TiO_2-silica membrane materials, Microporous Mesoporous Mater.221 (2016) 81-90.

[40]A. Farsi, S.H. Jensen, P. Roslev, V. Boffa, M.L. Christensen, Inorganic membranes for the Recovery of effluent from municipal wastewater treatment plants, Ind. Eng. Chem. Res. 54 (2015) 3462-3472.

[41]W.R. Bowen, J.S. Welfoot, Modelling the performance of membrane nano-filtration: critical assessment and model development, Chem. Eng. Sci. 57(2002) 1121-1137.

[42] B. E. Conway, Ionic Hydration in Chemistry and Biophysics, Elsevier Scientific Pub.

[43]K. Li, Ceramic membranes for separation and reaction, John Wiley&Sons Ltd,2007, pp. pp.22-28.

[44]W.B.S. de Lint, N.E. Benes, Separation properties of γ-alumina nanofiltration membranes compared to charge regulation model predictions, J. Membr. Sci.248 (2005) 149-159.

[45]G. Aryanpour, M.H. Abbasi, Computer simulation of ordinary gas transfer in tubes, J. Porous Media 8 (2005) 379-391.

[46]N.E. Benes, Mass Transport in Thin Supported Silica Membranes, University of Twente, Enschede, 2000. Ph.D. Thesis.

[47]T. Kuzniatsova, M.L. Mottern, K. Shqau, D. Yu, H. Verweij, Micro-structural optimization of supported γ-alumina membranes, J. Membr. Sci. 316 (2008) 80-88.

[48]Y.T. Chua, C.X.C. Lin, F. Kleitz, X.S. Zhao, S. Smart, Nanoporous organosilica membrane for water desalination, Chem. Commun. 49 (2013) 4534-4536.

[49]E. Chibowski, A. Szczes, L. Hołysz, Changes of zeta potential and particles sizeof silica caused by DPPC adsorption and enzyme phospholipase A2 presence, Adsorption 16 (2010) 305-312.

[50]V. Boffa, J.E. ten Wehner Elshof, D.H.A. Blank, Preparation of templated mesoporous silica membranes on microporous α-alumina supports via direct coating of thixotropic polymeric sols, Microporous Mesoporous Mater 100 (2007) 173-182.

[51]V. Boffa, G. Magnacca, L.B. Jørgensen, A. Wehner, A. D€ornh€ofer, Y. Yue, Towardthe effective design of steam-stable silica-based membranes, Microporous Mesoporous Mater 179 (2013) 242-249.

[52]S. Wijaya, M.C. Duke, J.C. Diniz da Costa, Carbonised template silica mem-branes for desalination, Desalination 236 (2009) 291-298.

[53]B.P. Ladewig, Y.H. Tan, C.X.C. Lin, K. Ladewig, J.C. Diniz da Costa, S. Smart Preparation, characterization and performance of templated silica membranesin non-osmotic desalination, Materials 4 (2011) 845-856.

[54]Y.F. Gu, S.T. Oyama, Permeation properties and hydrothermal stability of sil-icaetitania membranes supported on porous alumina substrates, J. Membr.Sci. 345 (2009) 267-275.

[55]V. Boffa, H.L. Castricum, R. Garcia, R. Schmuhl, A.V. Petukhov, D.H.A. Blank,J.E. ten Elshof, Structure and growth of polymeric niobia-silica mixed oxide sols for microporous molecular sieving membranes: a SAXS Study, Chem.Mater. 21 (2009) 1822-1828.

[56]V. Boffa, J.E. ten Elshof, R. Garcia, D.H.A. Blank, Microporous niobia-silica membranes: influence of sol composition and structure on gas transport properties, Microporous Mesoporous Mater. 118 (2009) 202-209

[57]C.J. Brinker, T.L. Ward, R. Sehgal, N.K. Raman, S.L. Hietala, D.M. Smith,D.W. Hua, T.J. Headley, Ultramicroporous silica-based supported inorganic membranes, J. Membr. Sci. 77 (1993) 165-179.

[58]V. Boffa, J.E. ten Elshof, D.H.A. Blank, Preparation of templated mesoporous silica membranes on microporous α-alumina supports via direct coating of thixotropic polymeric sols, Microporous Mesoporous Mater. 100 (2007) 173-182.

[59]K.S.W. Sing, D.H. Everett, R.A.W. Haul, L. Moscow, R.A. Pierotti, J. Rouquerol,T. Siemieniewska, Reporting physisorption data for gas/solid systems with special reference to the determination of surface area and porosity, Pure Appl.Chem. 57 (1985) 603-619.

[60]P. Olivier, Modeling physical adsorption on porous and nonporous solids using density functional theory, J. Porous Mater 2 (1995) 9-17.

[61]K.M. Mohiuddin, H.M. Zakir, K. Otomo, S. Sharmin, N. Shikazono, Geochemical distribution of trace metal pollutants in water and sediments of downstream of an urban river, Int. J. Environ. Sci. Tech. 7 (2010) 17-28.

[62]A. Musolff, S. Leschik, F. Reinstorf, G. Strauch, M. Schirmer, Micropollutant loads in the urban water cycle, Environ. Sci. Technol. 13 (2010) 4877-4883.

[63]J. Lienert, K. Gudel, B.I. Escher, Beate, Screening method for ecotoxicological hazard assessment of 42 pharmaceuticals considering human metabolism and excretory routes, Environ. Sci. Tech. 41 (2007) 4471-4478.

[64]I. Vergili, Application of nanofiltration for the removal of carbamazepine, diclofenac and ibuprofen from drinking water sources, J. Envir. Manag. 127(2013) 177-187.

[65]S. Beier, S. Koster, K. Veltmann, H.F. Schroder, J. Pinnekamp, Treatment ofhospital wastewater effluent by nanofiltration and reverse osmosis, Water Sci.Technol. 61 (2010) 1691-1698.

[66]X.M. Wang, L.B. Li, T. Zhang, X.Y. Li, Performance of nanofiltration membranein rejecting trace organic compounds: experiment and model prediction, Desalination 370 (2015) 7-16.

Table 1
Performance of commercial low-energy polymeric RO and NF membranes [4–15].

Membrane/Company	Type	ΔP [bar]	T [C]	pH	c_{NaCl}[a] [M]	Rec.[b] [%]	L_p [LMH bar^{-1}]	R_{NaCl} [%]	$R_{d\text{-}ion}$[c]
XLE-2521/DOW-FILMTEC [4]	RO	6.90	25	6–7	0.008	15	7.04	99	>99 $MgSO_4$
BW30-2540/DOW-FILMTEC [4]	RO	10.3	25	6–7	0.03	15	4.98	99.50	>99 $MgSO_4$
4040-ULP/KOCH [5]	RO	8.60	25	7.5	0.03	15	4.17	98.65	>99 $MgSO_4$
TMG10/TORAY [6]	RO	7.60	25	7	0.01	15	5.2–6.2	99	>99 $MgSO_4$
ESPA4-4040/HYDRANAUTICS [7]	RO	7.00	25	6.5–7	0.01	15	7.13	99.2	>99 $MgSO_4$
AK8040N 400/GE-DESAL [8]	RO	7.93	25	7.5	0.01	15	5.61	98	>99 $MgSO_4$
NF270/DOW-FILMTEC [9,10]	NF	4.8	25	6.5–7	0.016	15	10.5–10.85	>50	97 $MgSO_4$
NF90/DOW-FILMTEC [7,11]	NF	4.8	25	6.5–7	0.016–0.034	15	6.66–8.68	>85	97 $MgSO_4$
CK2540FM 30D/GE-DESAL [12]	NF	15.5	25	6.5	0.016	15	2.47	>50	94 $MgSO_4$
ESNA1-LF-LD/HYDRANAUTICS [13]	NF	5.2	25	6.5–7	0.004	15	6.70	>50	86-89 $CaCl_2$
8040-TS80-UWA/TRISEP [14]	NF	7.6	25	7–8	0.016	15	5.45	>50	97-99 $MgSO_4$
NE 8040-90/CSM[15]	NF	5	25	6.5–7	0.004–0.034	15	6.36	85–95	90-95 $CaCl_2$
NE 8040-70/CSM [15]	NF	5	25	6.5–7	0.004–0.034	15	5.9	40–70	45-70 $CaCl_2$

[a] Concentration of NaCl in the feed.
[b] Recovery.
[c] Retention of divalent ions.

Table 2
Desalination performance of inorganic NF and low UF membranes [24,29–36].

Membrane	Top layer	d_p [nm]	L [μm]	ΔP [bar]	T [°C]	pH	c_{NaCl} [M]	L_p [LMH bar^{-1}]	R_{NaCl} [%]
MFI Zeolite	Silicalite [29]	0.55	9.8	10	25	7.6	N/A	0.04	47
	Silicalite [30]	0.5–0.6	2	7	25		0.1	0.05	72
	ZSM-5 Si/Al = 65 [30]	0.5–0.6	2	7	25		0.1	0.02	84
	ZSM-5 Si/Al = 50 [30]	0.5–0.6	2	7	25		0.1	0.005	88
Organosilica	BTESE_100 [31]	0.5	0.2	7	25		0.03	0.11	89
	BTESE_300 [31]	0.5	0.2	7	25		0.03	0.06	96
	BTESE [24]	0.55	0.2	9	25	6–7	0.034	0.18	65
Titania	TiO_2 [32]	2	0.1	5		6–7	0.01	20	10–15
	TiO_2 [33]	0.55–2	0.05	6		6–7	0.01	20	38
	TiO_2 [34]	4	0.5	7	30	6.2	0.01	8	30
Zirconia	ZrO_2-400 [35]	1.8	N/A	6	25	6	0.01	0.3	20
	ZrO_2-350 [35]	0.94	N/A	6	25	6	0.01	0.2	22
Alumina	γ-alumina [36]	3.4	N/A	6	25	5.5–6	0.001	2	52
	γ-alumina [36]	8.7	4	6	25	5.5–6	0.001	11	40
	γ-alumina [24]	4.4	1.2	9	25	5.5–6	0.034	10–12	20

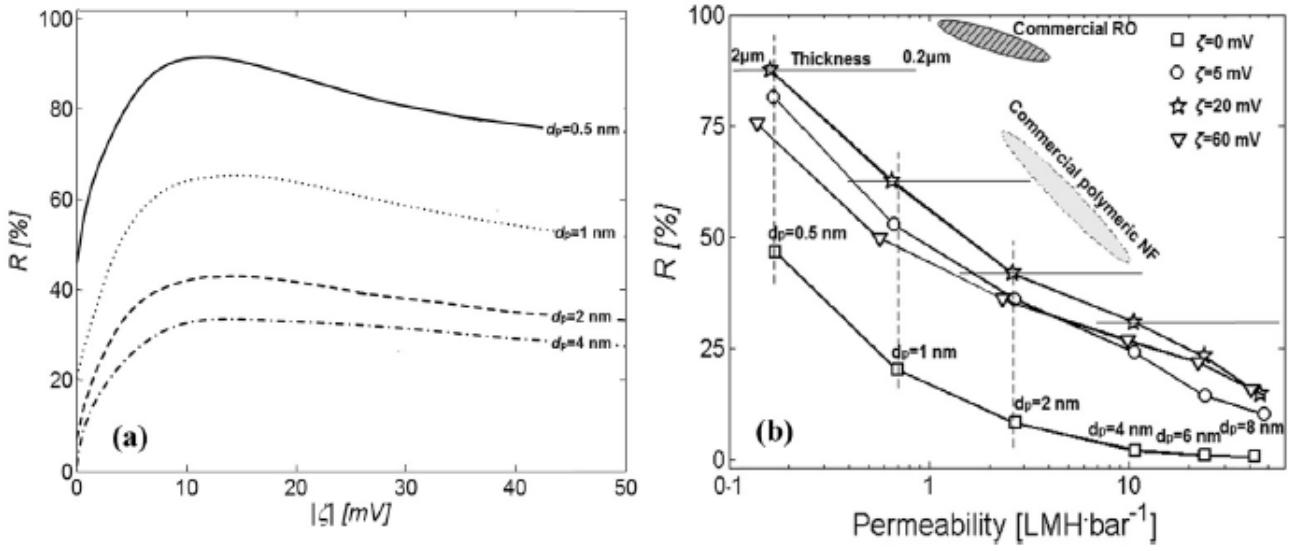

Fig. 1. (A) simulation of NaCl rejection (R) of porous membranes vs. z-potential for different pore sizes (d_p); (b) Permeability and NaCl rejection of porous membrane in different pore size and ζ-potential (ΔP = 6 bar, c_{NaCl} = 0.01 M, ε = 0.5, τ = 3, l = 1 μm, T = 25°C, black lines show the effect of membrane thickness on permeability between 2 μm and 0.2 μm, dash-lines was drawn to compare permeability for certain pore size).

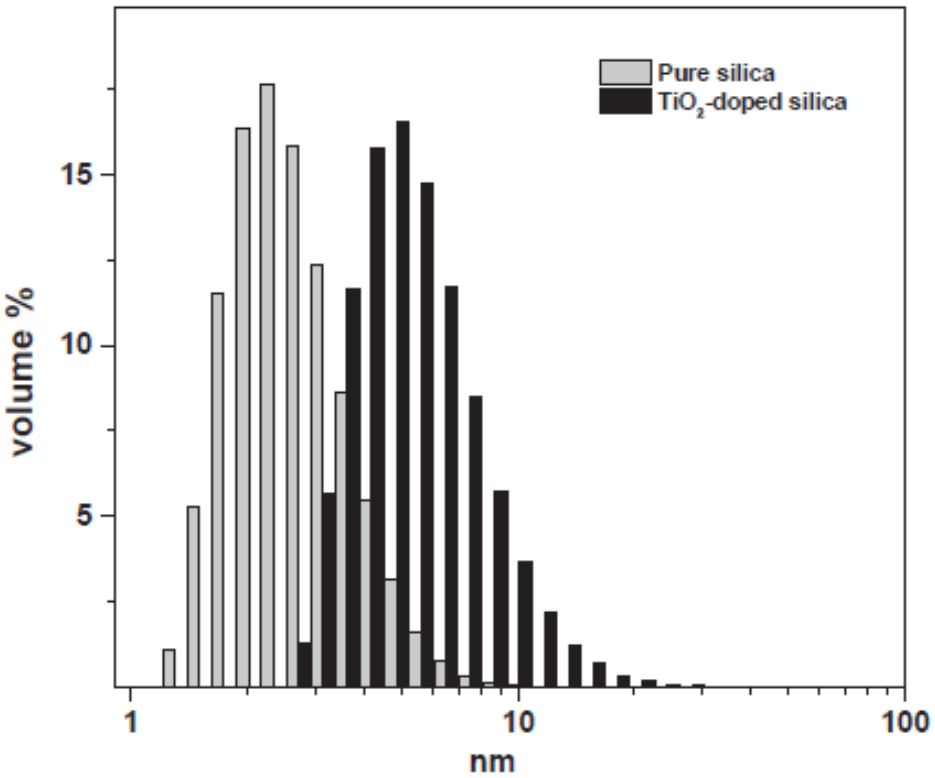

Fig. 2. Particle size distribution of the sols used for the coating of the pure silica and of the TiO_2-doped membranes, as measured by dynamic light scattering (DLS).

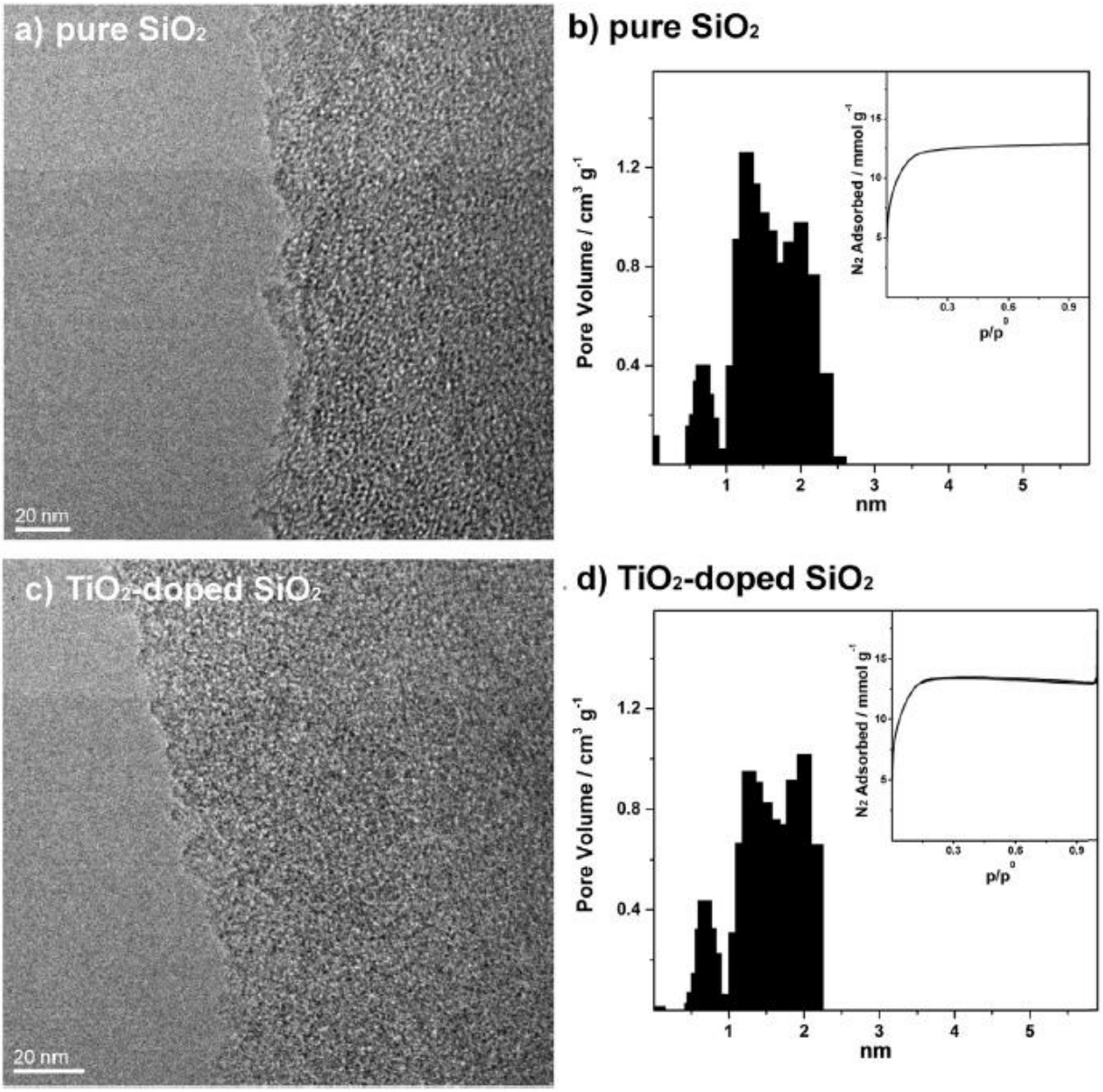

Fig. 3. TEM images of the unsupported pure silica (a) and TiO_2-doped (c) silica membranes, and the correspondent pore size distributions (b and d, respectively). Pore size distributions were calculated from the sorption isotherms in the insert by the DFT method [60].

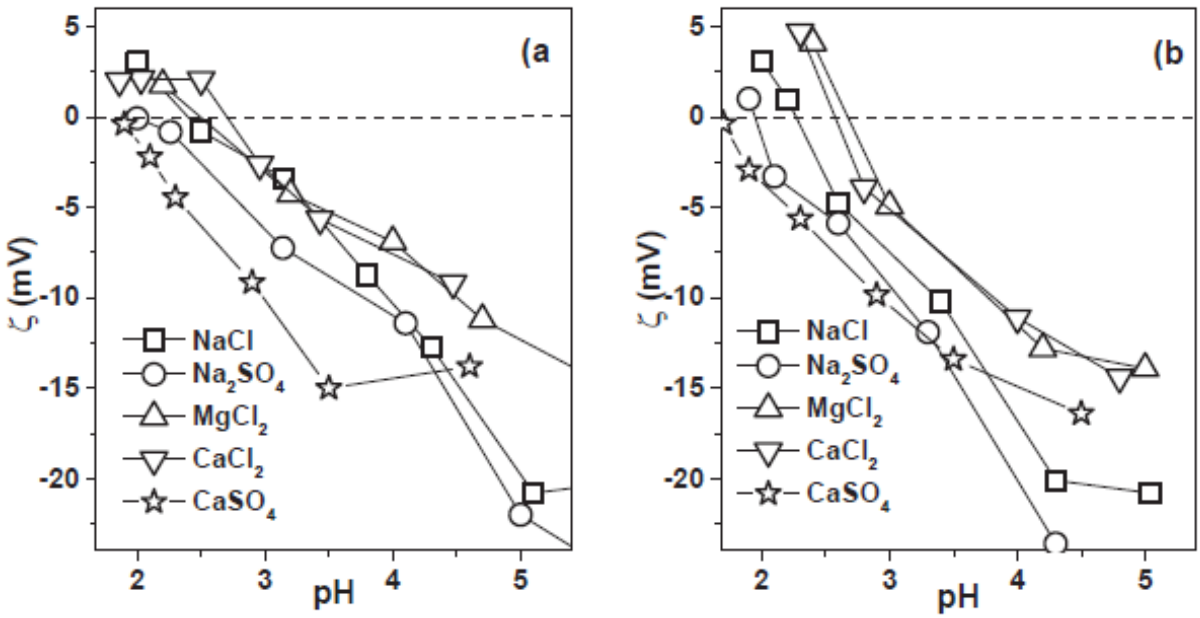

Fig. 4. ζ-potential vs pH graphs for a pure silica reference sample and a 5% TiO_2-doped silica unsupported membrane (ionic strength 0.01 M).

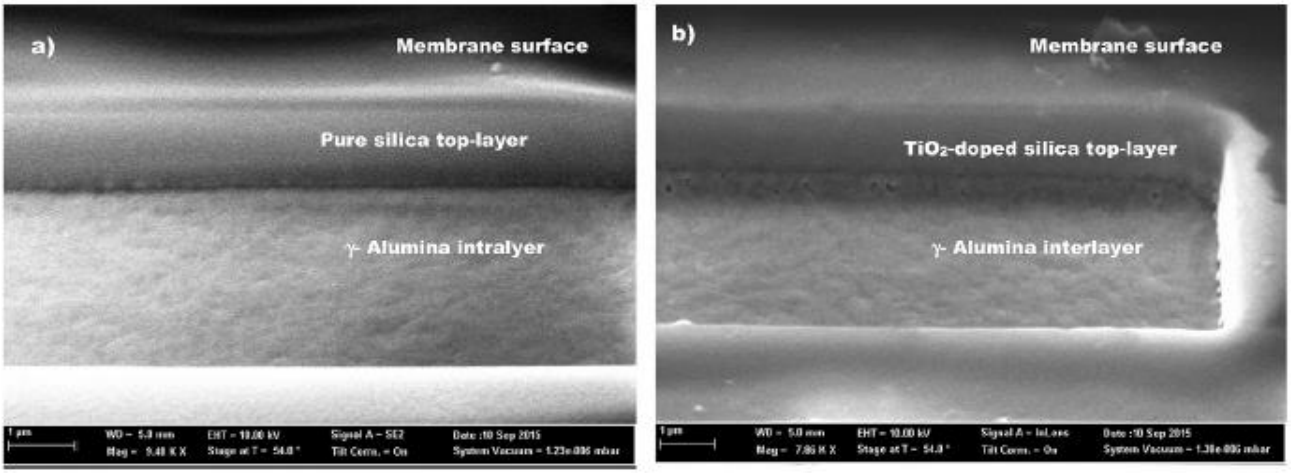

Fig. 5. SEM cross-section image of the pure silica and of the 5%TiO_2-doped silica membranes. The micrographs show the membrane active layer and the γ-alumina interlayer. Membrane cross-sections were realized by FIB (Focused Ion Beam).

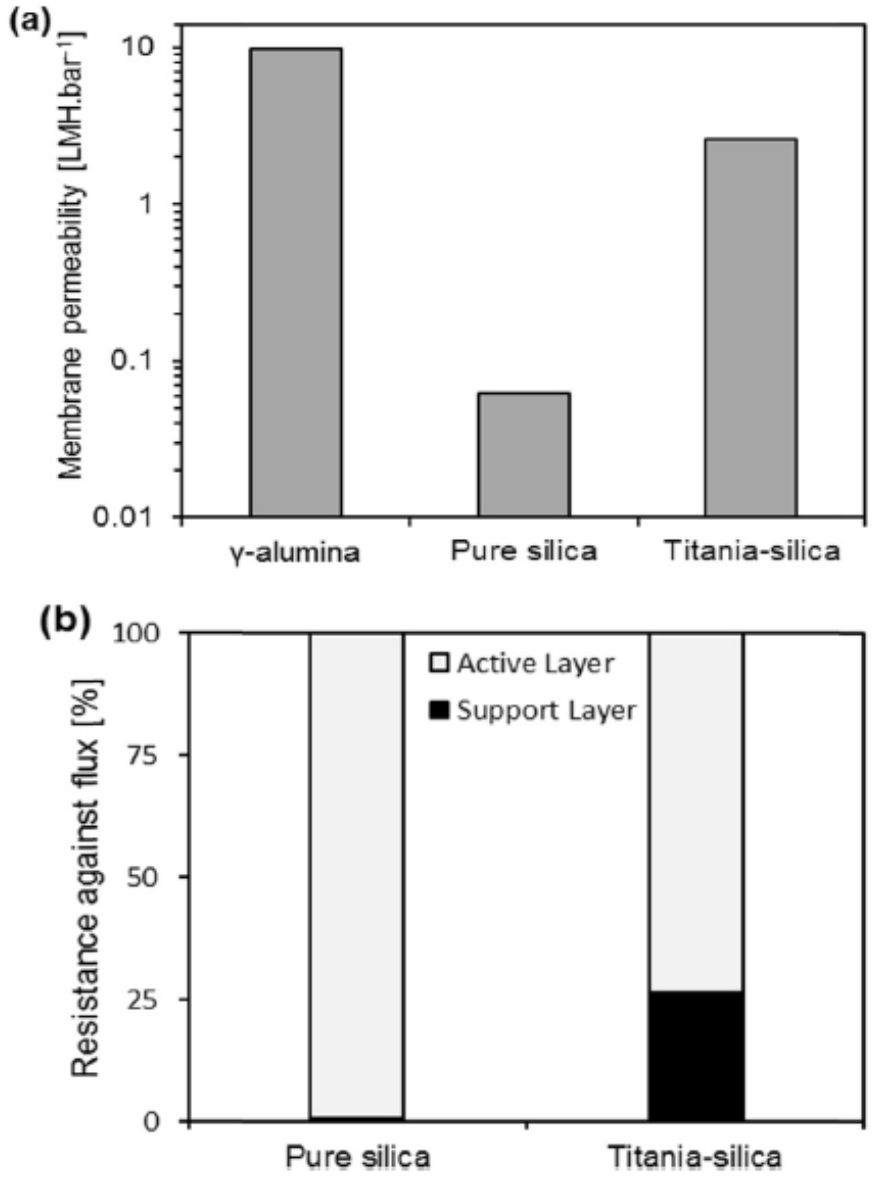

Fig. 6. Membrane permeabilities (a) and contribution to the resistance against the water flux (b) of the γ-alumina carrier, of the pure silica membrane and of the 5%TiO_2-doped silica membrane.

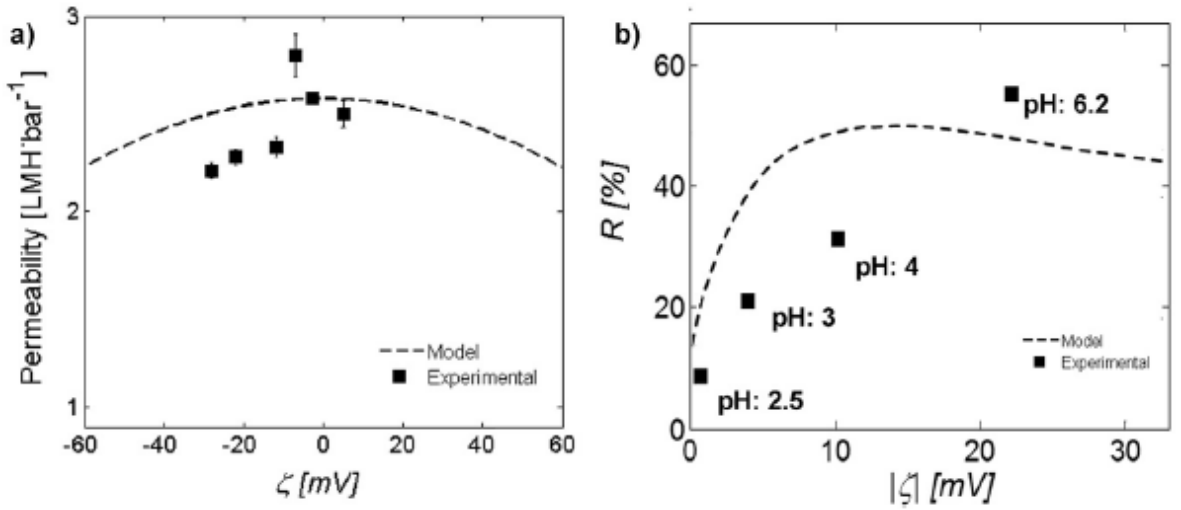

Fig. 7. Water permeability (a) and NaCl rejection (b) of the 5% TiO_2-doped silica membrane vs. ζ (ΔP = 6 bar, c_{NaCl} = 0.01 M and T = 25°C, dash line shows the model prediction (d_p = 1.44 nm, l = 1.2 μm, ε = 0.71).

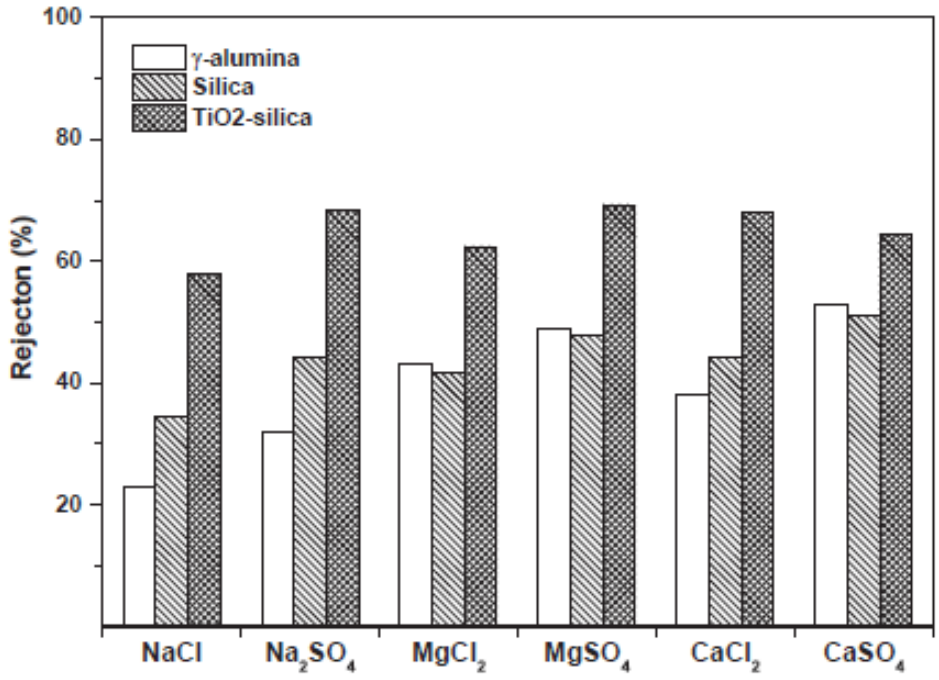

Fig. 8. Salt rejection of the pure silica membrane and the TiO2-doped silica membrane compare with the γ-alumina support (ΔP = 6 bar, ionic strength for all solutions was 0.01 M and T = 25°C).

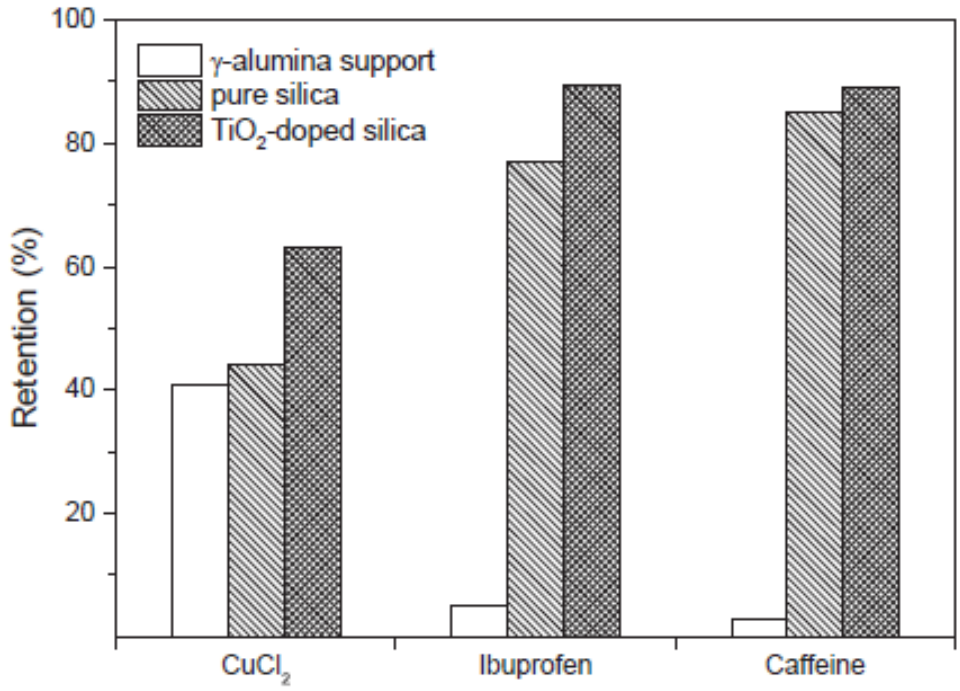

Fig. 9. Retention of the γ-alumina support, of the pure silica membrane and of the 5% TiO_2-doped membrane to three model pollutants: $CuCl_2$, ibuprofen and caffeine.